PHYSICAL REVIEW B

CONDENSED MATTER

THIRD SERIES, VOLUME 32, NUMBER 11 1 DECEMBER 1985

Spin dynamics in Ni near T_C: A high-resolution neutron scattering study

J. L. Martínez,* P. Böni, and G. Shirane
Brookhaven National Laboratory, Upton, New York 11973
(Received 3 June 1985)

We have studied the magnetic cross section in Ni below and above T_C using unpolarized and polarized neutron scattering techniques. For temperatures near the Curie temperature ($T_C=631$ K) and for a range of momentum transfer $0.2<q<0.4$ Å^{-1} (Brillouin zone width$\simeq$1.54 Å^{-1}), the spin waves renormalize as expected from extrapolating the results at smaller momentum transfer ($q<0.2$ Å^{-1}). At T_C the spin waves merge into a broad single peak centered at zero-energy transfer, which is well described by a double-Lorentzian scattering function. Our results, below and above T_C, agree with the predictions of the dynamic scaling theory in the area of (q,ω) space and the range of temperatures investigated. This is in contrast with recent measurements which reported magnetic excitations at finite energies above T_C.

I. INTRODUCTION

The magnetic properties of the transition metals are still an unresolved problem in magnetism. Amongst these, Fe and Ni are the most celebrated examples and their properties have been widely studied by means of many experimental techniques and theoretical work. One of the most powerful means to study the magnetic properties is inelastic neutron scattering and several experiments have been performed in the last few years.[1–6] In an early work Minkiewicz *et al.*[1] studied the renormalization of the spin waves in Ni for q values smaller than 0.2 Å^{-1} at different temperatures below T_C and the diffuse scattering above T_C. Just below the Curie temperature, spin waves become critically overdamped and there is a continuous evolution to critical scattering at T_C. Figure 1 illustrates quadratic dispersion curves at different temperatures, calculated using values of the stiffness constant D, from Ref. 1. Recently, Steinsvoll *et al.*[3] extended the range of the measurements up to $q\simeq 0.4$ Å^{-1} for $T>T_C$, showing that the main part of the magnetic scattering has the form of a broad Lorentzian centered at zero-energy transfer.

In contrast to Ni the spin dynamics near T_C of Fe have been extensively studied. In an early work[7] the magnetic scattering from Fe for small q values was measured for temperatures near T_C. The results were in agreement with the dynamic scaling predictions and later on this study was extended to higher q values ($q<0.26$ Å^{-1}), below and above T_C,[8] showing a close correspondence with earlier measurements made at smaller momentum transfers. Finally, magnetic scattering cross sections were characterized[9] for bcc Fe above T_C in a q range of 0.1–0.6 Å^{-1}.

For comparison to the itinerant ferromagnets, it would be interesting to compare the behavior of typical localized Heisenberg cubic ferromagnets like EuO or EuS with the itinerant systems. EuO and EuS are the only known isotropic cubic ferromagnets which exhibit peaks at finite energy[10–12] near the zone boundary. This shows unambiguously that propagating modes are present in the paramagnetic phase. However, in an intermediate range of q values the behavior is similar to that reported for other isotropic cubic ferromagnets like the localized metallic system[13] Pd_2MnSn or the itinerant metallic systems[3–5,9] Ni and Fe.

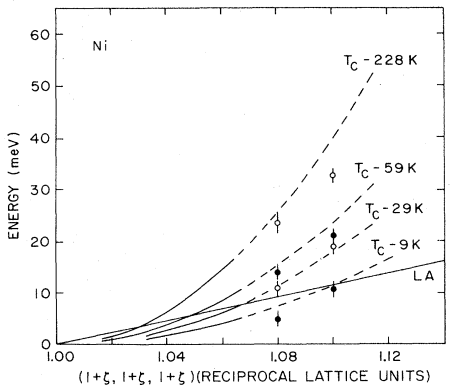

FIG. 1. Magnon dispersion curves at different temperatures calculated from Ref. 1 (solid curves), and extrapolated to higher q values (dashed curves). Circles are the peak positions in constant-Q scans at different temperatures of the present study. LA is the longitudinal-acoustic–phonon branch.

A careful examination of the magnetic scattering from Ni below and above T_C, at the intermediate q range ($0.2 < q < 0.4$ Å^{-1}) is urgently needed. This is, no doubt, stimulated by the recent controversy concerning propagating spin wave above T_C,[2-6] as we shall discuss in detail later. Equally important is the lack of the proper characterization of the scattering function below T_C for this important q range. Actually the work of Minkiewicz *et al.* was done before the full development of the dynamic scaling theory; thus our data analysis can be performed using the more detailed theories developed since the important work of Minkiewicz *et al.*

In this paper we shall present high-resolution polarized and unpolarized neutron scattering data below and above T_C. The renormalization of the spin waves, at different temperatures below T_C, will be investigated in order to characterize the scattering function. Finally, we shall discuss how the double-Lorentzian expression, for the paramagnetic scattering function, centered at zero-energy transfer gives the most consistent picture for the available experimental data in Ni.

II. EXPERIMENTAL TECHNIQUE

The experiments were performed on an isotopically enriched single crystal of ^{60}Ni of cylindrical shape with a volume of 2.9 cm^3. The inverse of the distance between nearest (111) planes at T_C was equal to 3.09 Å^{-1} (lattice constant $a = 3.53$ Å). With this particular choice of the isotope, nuclear-spin and isotopic incoherent scattering are drastically reduced. The data were collected around the (111) Bragg point in the [111] direction. The crystal was heated in a vacuum furnace, specially designed to avoid stray fields generated from the heater currents, which could depolarize the beam. The temperature was measured with a Chromel-Alumel thermocouple directly attached to the sample. The stability of the temperature reading was ± 0.5 K over long periods of time. The Curie temperature of the sample was determined by measuring the critical diffuse magnetic scattering for a small q value of 0.06 Å^{-1}, setting the spectrometer at zero-energy transfer. We confirmed T_C also by measuring the depolarization of the polarized neutron beam by the sample on cooling. Both measurements gave a consistent result $T_C = 631$ K.

Neutron scattering measurements were performed on triple-axis spectrometers at the Brookhaven High Flux Beam Reactor. Various experimental configurations were tried since it is always a challenge for neutron scattering experimentalists to find the best experimental condition giving the necessary intensity and the desired resolution. In particular, Ni is a difficult case because of the small paramagnetic magnetic moment[3] ($\mu_{\text{eff}}^2 = 2.58\mu_B^2$) and, consequently, the weak signal. In Table I we show the values, full width at half maximum (FWHM), of the projections of the resolution ellipsoid on the q_x, q_y, q_z, and E axes for our present experimental configurations as well as for the recent experiments of Mook and Lynn.[6] The figure of merit R is proportional to the overall volume of the resolution ellipsoid with the 14.7-meV setup taken as $R \equiv 1$.

In the unpolarized neutron experiments pyrolitic graphite (PG) was used as monochromator and analyzer and a PG filter was used to remove higher-order contamination. For the polarization analysis, Heusler (111) crystals were used in transmission geometry as monochromator and analyzer. Experimental details of the polarization-analysis technique and the polarized beam setup have been reported previously.[5,9,13]

III. MAGNETIC SCATTERING FROM NICKEL

The general form for the magnetic cross section can be written as

$$\frac{d^2\sigma}{d\Omega\, d\omega} = \frac{k_f}{k_i}\gamma_0^2 |f(Q)|^2 S(q,\omega) , \tag{1}$$

where the dynamical structure factor $S(q,\omega)$ is the Fourier transform of the spin pair correlation function, k_i and k_f are the incident and final wave vectors of the neutrons, $\gamma_0^2 = 0.291$ b/sr, and $f(Q)$ is the atomic magnetic form factor. Below T_C, considering only the spin waves,

$$S(q,\omega) \propto \chi(q) \frac{\hbar\omega}{1-\exp(-\hbar\omega/k_B T)} F(q,\omega) \tag{2}$$

with the shape function

$$F(q,\omega) = \frac{1}{2\pi}\left[\frac{\Gamma}{(\omega_q-\omega)^2-\Gamma^2} + \frac{\Gamma}{(\omega_q+\omega)^2+\Gamma^2}\right] . \tag{3}$$

$F(q,\omega)$ has poles at $\hbar\omega_q = \pm Dq^2$, with the half-width at half maximum (HWHM) Γ. The susceptibility $\chi(q)$ below T_C is independent of temperature and proportional to $1/q^2$.

TABLE I. Specifications of the resolution parameters for our experimental setups as well as those from Ref. 6. All the calculations are made for an energy transfer of 20 meV. The projection of the resolution ellipsoid on the three momentum axes (FWHM) are given in Å^{-1}, and on the energy axis (FWHM) in meV. R is proportional to the overall volume of the resolution ellipsoid.

	Collimation (min)	Monochromator	E_f (meV)	Δq_x (Å^{-1})	Δq_y (Å^{-1})	Δq_z (Å^{-1})	ΔE (meV)	R
Present work	40′-20′-40′-20′	PG[a]	14.7	0.029	0.123	0.12	1.940	1
Present work	40′-60′-40′-60′	Heusler[b]	30.5	0.067	0.320	0.16	6.089	25
Mook and Lynn[c]	40′-40′-40′-120′	^{57}Fe[b]	40	0.068	0.205	0.19	4.166	13
Mook and Lynn[c]	40′-40′-40′-120′	^{57}Fe[b]	60	0.080	0.296	0.23	7.034	46

[a]Unpolarized neutron beam.
[b]Polarized neutron beam.
[c]Reference 6.

In the paramagnetic region ($T \geq T_C$) the susceptibility becomes, for small q values,

$$\chi(q)=\chi(0)\frac{\kappa_1^2}{\kappa_1^2+q^2} . \quad (4)$$

Here $\chi(0)$ is the static susceptibility. The spectral weight function is usually approximated by

$$F(q,\omega)=\frac{1}{\pi}\left[\frac{\Gamma}{\Gamma^2+\omega^2}\right], \quad (5)$$

where the quasielastic linewidth (HWHM) is

$$\Gamma=Af(\kappa_1/q)q^{2.5} . \quad (6)$$

$f(\kappa_1/q)$ is a dynamical scaling function and κ_1 is the inverse correlation length.

A. Unpolarized neutron beam

Let us first present the results of the renormalization of the spin waves in Ni for temperatures approaching T_C. Figure 2 shows constant-Q scans for (1.08,1.08,1.08), $q \simeq 0.25$ Å^{-1}, at two different temperatures. Well below the Curie temperature T_C [Fig. 2(b)], the scan clearly shows a magnon peak well separated from the longitudinal-acoustic (LA) phonon and the incoherent scattering which appear as very sharp and narrow peaks. At 5 meV some intensity appears from the transverse-acoustic (TA) phonon because of the finite resolution. The solid line is a fit to the data using Eqs. (1)—(3) convoluted with the instrumental resolution function. In the cross section we have not included a longitudinal component for the susceptibility because it is expected to be small. The fitted values obtained for $q \simeq 0.25$ Å^{-1} are $D=422\pm5$ meV Å^2 and $\Gamma=4.37$ meV, where D is the spin-wave-stiffness constant and Γ is the linewidth. The value of D from Minkiewicz *et al.* for this temperature is $D=417$ meV Å^2, which agrees very well with our value. A constant background was assumed for this fit, as shown by the horizontal dashed line.

In the experimental configuration used above, a pyrolitic graphite filter was placed after the sample and a correction has been made because higher-order neutrons are also detected at the monitor counter, which is placed after the monochromator. These contaminating neutrons are counted with a steadily decreasing efficiency proportional to $1/k_i$ at the monitor detector. The correction increases with decreasing E_i reaching about one-third at 15 meV whereas above 30 meV it is negligible. Nevertheless, it can be calibrated accurately either by measuring phonon and magnon intensities and comparing them with theoretical cross sections, or by using transmission measurements through boron glass attenuators.[14]

Unpolarized neutron measurements were also performed above T_C as shown in Fig. 2(a). The data was fitted to Eq. (1) using Eqs. (4)—(6) and convoluted with the instrumental resolution. The solid line in Fig. 2(a) is the result of the fit and we obtained $Af(\kappa_1/q)=226\pm8$ meV Å$^{5/2}$.

In this figure, the contributions from TA and LA phonons have been subtracted. However, the data points at 0 and 10 meV have been omitted because their intensity can not be subtracted reliably. For these calculations a constant background, identical to the low-temperature data, was assumed. The agreement between experimental data and the fits is very good.

From the low-temperature data we should be able to follow the renormalization of the magnon peaks with increasing temperature. The magnon should become broad and finally merge into a quasielastic peak at zero-energy transfer. This behavior is shown in Fig. 3 for

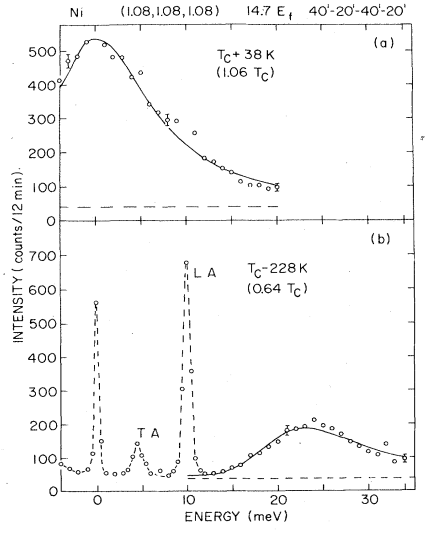

FIG. 2. Constant-Q scans at (1.08,1.08,1.08), $q \simeq 0.25$ Å^{-1}, for two different temperatures (a) $1.06T_C$ and (b) $0.64T_C$. Solid curves are fits using the corresponding spectral weight functions as explained in the text. The horizontal dashed lines show the estimated background level.

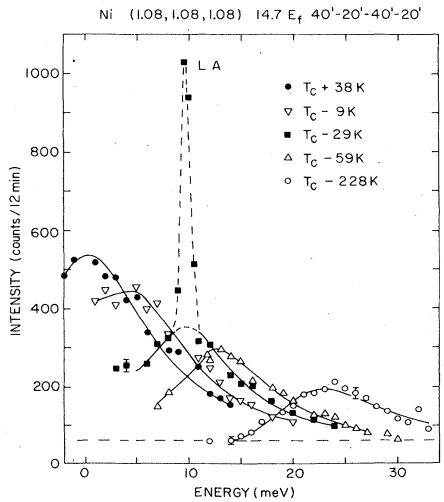

FIG. 3. Magnetic scattering from nickel at different temperatures for (1.08,1.08,1.08), $q \simeq 0.25$ Å^{-1}. Also shown is the LA phonon at T_C-29 K. The solid curves are fits as explained in the text.

(1.08,1.08,1.08). The dashed line shows the LA phonon for T_C-29 K; for this temperature the LA dispersion curve coincides with the spin-wave dispersion curve. The solid curves are fits using Eqs. (1)—(3). The fitted values of D for each temperature are in agreement with the extrapolated values from Minkiewicz *et al.*, as is shown in Fig. 1. In this figure, the magnon peak positions for $\zeta=0.08$ are plotted as well as the dispersion curves for the corresponding temperature calculated from the data in Ref. 1 and extrapolated to the present q position using the quadratic form $\hbar\omega_q=Dq^2$. The agreement between extrapolations and experimental data is good.

Figure 4 represents constant-Q scans for $\zeta=0.10$ ($q\simeq 0.31$ Å^{-1}) measured at the same temperatures as in Fig. 2. Below T_C, Fig. 4(b), the magnon peak is clearly separated from the phonon peaks and the incoherent scattering. The solid line is a fit using Eqs. (1)—(3). The fitted parameters are $D=412\pm 9$ meV Å^2 and $\Gamma=9.2$ meV. The background was assumed at the level of the horizontal dashed line. It was not possible to extend the measurements to higher-energy transfers to completely measure the magnon peak because of momentum- and energy-conservation laws. Figure 4(a) illustrates the paramagnetic scattering ($1.06T_C$) for this q value. Again, experimental data points at the peak positions of the LA phonon and the incoherent peaks have been omitted and the intensity corresponding to the LA and TA phonons has been subtracted. The experimental data have been fitted to Eq. (1) using Eqs. (4)—(6) and we obtain $Af(\kappa_1/q)=248\pm 18$ meV Å$^{5/2}$.

Figure 5 illustrates the renormalization of the spin waves on approaching T_C from below for (1.1,1.1,1.1). The values of the peak position for different temperatures are plotted in Fig. 1. The agreement with the extrapolated curves is good. The slight deviations observed are expected to become significant at higher q values because the simple quadratic behavior fails. No peaks at finite energies can be observed in Figs. 2 and 5 for $T>T_C$. The scattering is quasielastic, in agreement with all our previous measurements and in disagreement with those of Ref. 6.

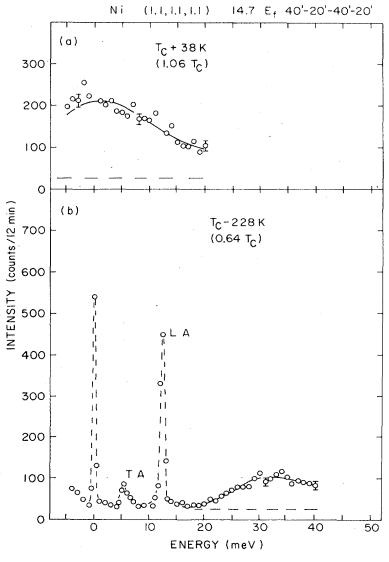

FIG. 4. Constant-Q scans at (1.1,1.1,1.1), $q\simeq 0.31$ Å^{-1}, for two different temperatures (a) $1.06T_C$ and (b) $0.64T_C$. Solid curves are fits using Eqs. (1)—(6). The horizontal dashed lines are the background levels.

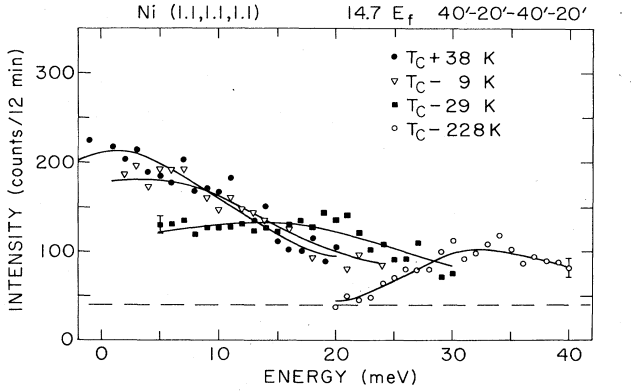

FIG. 5. Renormalization of the spin waves at different temperatures for (1.1,1.1,1.1), $q\simeq 0.31$ Å^{-1}. The solid curves are fits using Eqs. (1)—(6).

From the unpolarized neutron scattering data above T_C we have determined the absolute cross sections, which agree within 15% with those determined from polarized beam experiments. The study of the paramagnetic scattering with unpolarized neutrons is limited to the specific cases where it is possible to isolate all background contributions. Then, unpolarized neutrons are more useful because of the better resolution and higher intensity. In other cases, the polarization analysis technique is a more effective way to measure the paramagnetic scattering from isotropic ferromagnets.

B. High-resolution polarized beam results above T_C

In neutron scattering experiments with weak signals the most uncertain element is the background, which comes from room background and everything in the beam path including the sample. Moreover, when constant-Q scans with fixed final energy are performed the counting time can easily differ by a factor of 2 for large energy transfers due to the reduced neutron flux at higher energies. Thus, a realistic estimation of the background is very difficult. Therefore the use of polarized neutrons taking the difference between intensities with the neutron polarization parallel to **Q** ($I_{\rm HF}$) and perpendicular to **Q** ($I_{\rm VF}$) (HF and VF denote horizontal and vertical magnetic field, respectively) is essential to obtain reliable data[9,15] since all the nonmagnetic "background" cancels out in the subtraction. The results for the paramagnetic scattering on Ni using the difference technique are described in this section.

In Fig. 6 we present constant-Q scans at $1.06T_C$. Open circles in Fig. 6(a) show the paramagnetic scattering for $\zeta=0.10$ ($q\simeq 0.31$ Å^{-1}), where $\zeta=0.50$ corresponds to the zone boundary [see Fig. 4(a) for the unpolarized results at the same temperature and q]. The solid curve is calculated from Eqs. (1) and (4)—(6), and convoluted with

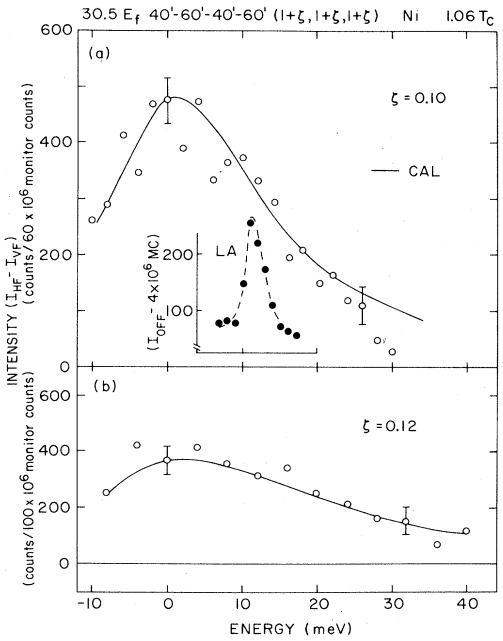

FIG. 6. Paramagnetic scattering for (a) $\zeta=0.10$ ($q\simeq 0.31$ Å^{-1}) and (b) $\zeta=0.12$ ($q\simeq 0.37$ Å^{-1}). Solid curves are calculations using Eqs. (1) and (4)—(6). The inset shows the longitudinal-acoustic phonon measured with flipper off, to demonstrate the good resolution of the experimental setup.

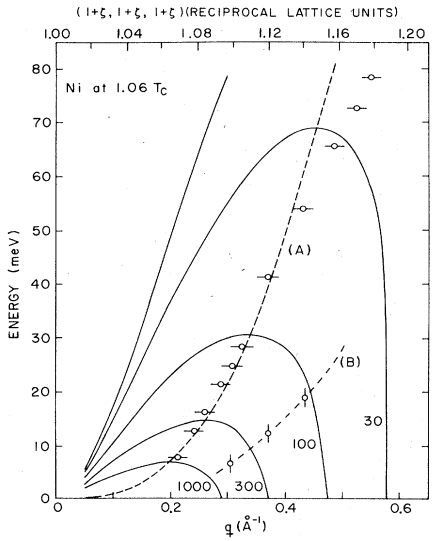

FIG. 7. Equal-intensity contours calculated with $\alpha=0.01$, $\kappa_1=0.09$ Å^{-1}, and $A=350$ meV Å$^{2.5}$; dashed curve (A) corresponds to the "dispersionlike" curve for constant-energy scans. Open circles with a horizontal bar are the peak positions in constant-energy scans from Ref. 2. Open circles with a vertical bar are the values of ω_0 in constant-Q scans from Ref. 6. Dashed curve (B) is just a guide to the eye.

the resolution function. In this case we have assumed for $f(\kappa_1/q)$ the scaling function obtained by Résibois-Piette[16] [$f(\kappa_1/q)=0.64$], and $A=350$ meV Å$^{5/2}$. The only free parameter, the normalization constant, used in this calculation has been estimated from the magnetic cross sections around zero-energy transfer. These data clearly demonstrate that the paramagnetic scattering is centered at zero-energy transfer or, in other words, the intensity at $\Delta E=0$ is significantly higher than at any other energy in the measurement range. The inset of Fig. 6(a) shows the LA phonon measured with flipper off and HF on. This configuration is sensitive to the nuclear scattering but not to the magnetic one. The energy width of the phonon indicates the energy resolution and as seen, it is much narrower than the width of the quasielastic scattering. Figure 6(b) illustrates the data for $\zeta=0.12$. Again the solid line is calculated from the Eqs. (1) and (4)—(6), using the normalization constant from Fig. 6(a), properly scaled by the monitor factor.

IV. DISCUSSION

We have measured the magnetic cross section in Ni for an important intermediate range of q, with high-resolution neutron scattering techniques. Our unpolarized measurements demonstrate how peaks at finite energy, below T_C, evolve into a single peak at T_C. We have also employed a high-resolution polarized beam technique that reconfirms our previous results,[3-5] which were interpreted in terms of a double-Lorentzian scattering function (see Fig. 6). A modification of the Lorentzian spectral weight function has been proposed[5,9] in order to better explain the constant-energy peak positions. Figure 7 illustrates calculated constant-energy peak positions [dashed curve (A)] as well as equal-intensity contours using the modified double Lorentzian for $T=1.06T_C$. Open circles with a horizontal bar are the peak positions as measured in constant-energy scans, from Ref. 2. Recently, Folk and Iro[17] have studied the paramagnetic scattering in isotropic

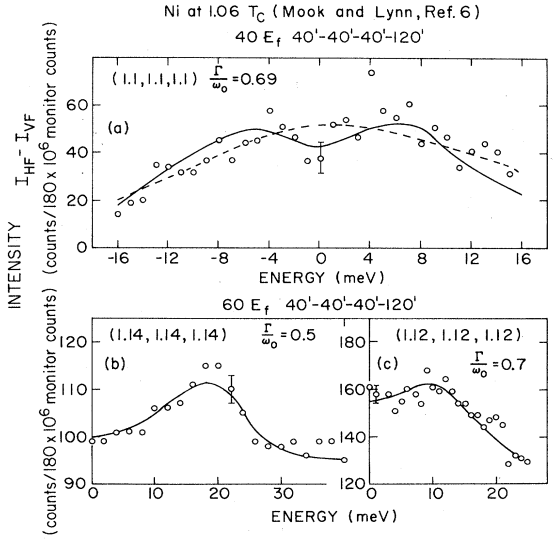

FIG. 8. (a) Open circles and solid curves are reproduced from Fig. 6 of Ref. 6. Dashed curve is the fit with Eqs. (1) and (4)—(6) yielding $Af(\kappa_1/q)=325\pm 38$ meV Å$^{2.5}$. (b) and (c) Experimental data and fits with a damped harmonic oscillator from Fig. 5 of Ref. 6, for $\zeta=0.14$ and 0.12, respectively.

ferromagnets by renormalization-group theory. They found complete agreement between experiment and theory for the positions of the constant-energy peaks.

Recently, new data for the paramagnetic scattering from Ni have been reported[6] which have been interpreted as propagating spin waves. The measured peak positions are indicated in Fig. 7 as open circles with a vertical bar. These new data form a "dispersionlike" curve [curve (B)] at much lower energy than the one previously reported.[2] These propagating spin waves above T_C are not observed in our current measurements (see Fig. 6). We do not understand why these different cross sections are observed. It is definitely not the resolution effect, as hinted in Ref. 6, since our current resolutions are equivalent to theirs in the polarized setup and considerably better in the unpolarized case.

The only data from Ref. 6 obtained by the polarization-analysis technique I_{HF}-I_{VF} are shown in Fig. 8(a). The data can be fitted equally well either with a damped harmonic oscillator as used in Ref. 6 (solid line) or a single Lorentzian (dashed line); thus these data cannot be regarded as evidence of propagating spin waves. The rest of the data from Ref. 6 have been obtained by applying a horizontal magnetic field (HF) with flipper on (no full polarization analysis), Figs. 8(b) and (c). These seem to show very large peaks, but actually they are very small if one realizes that the zeros of the intensity have been suppressed. We do not understand the discrepancies between our data and those of Ref. 6; therefore a joint experiment would be very enlightening.

In summary, we have shown that in Ni the spin waves renormalize, in an intermediate range of momentum transfer, as expected from scaling laws. The temperature dependence of the stiffness D agrees well with the results of Ref. 1 from measurements at small q values. However, the linewidth of the spin waves, Γ, has not yet been quantitatively characterized and more accurate experiments are planned in the near future, in order to get the exact expression for the renormalization of Γ below T_C.

ACKNOWLEDGMENTS

The authors would like to thank P. W. Mitchell, T. Moriya, S. M. Shapiro, Y. J. Uemura, and J. P. Wicksted for many helpful discussions. Work at Brookhaven National Laboratory was supported by the Division of Materials Sciences, U.S. Department of Energy, under Contract No. DE-AC02-76CH00016.

*Permanent address: Departamento de Optica C-4, Universidad Autónoma de Madrid, 28049 Madrid, Spain.

[1]V. J. Minkiewicz, M. F. Collins, R. Nathans, and G. Shirane, Phys. Rev. **182**, 624 (1969).

[2]H. A. Mook, J. W. Lynn, and R. M. Nicklow, Phys. Rev. Lett. **30**, 556 (1973); J. W. Lynn and H. A. Mook, Phys. Rev. B **23**, 198 (1981).

[3]O. Steinsvoll, C. F. Majkrzak, G. Shirane, and J. Wicksted, Phys. Rev. Lett. **51**, 300 (1983); O. Steinsvoll, C. F. Majkrzak, G. Shirane, and J. Wicksted, Phys. Rev. B **30**, 2377 (1984).

[4]Y. J. Uemura, G. Shirane, O. Steinsvoll, and J. Wicksted, Phys. Rev. Lett. **51**, 2322 (1983).

[5]P. Böni and G. Shirane, J. Appl. Phys. **57**, 3012 (1985).

[6]H. A. Mook and J. W. Lynn, J. Appl. Phys. **57**, 3006 (1985).

[7]M. F. Collins, V. J. Minkiewicz, R. Nathans, L. Passell, and G. Shirane, Phys. Rev. **179**, 417 (1969).

[8]S. Boronkay and M. F. Collins, Int. J. Magn. **4**, 205 (1973).

[9]J. P. Wicksted, P. Böni, and G. Shirane, Phys. Rev. B **30**, 3655 (1984).

[10]H. A. Mook, Phys. Rev. Lett. **46**, 508 (1981).

[11]H. G. Bohn, A. Kollmar, and W. Zinn, Phys. Rev. B **30**, 6504 (1984).

[12]P. Böni and G. Shirane (unpublished).

[13]G. Shirane, Y. J. Uemura, J. P. Wicksted, Y. Endoh, and Y. Ishikawa, Phys. Rev. B **31**, 1227 (1985).

[14]R. A. Cowley, G. Shirane, R. J. Birgeneau, and H. J. Guggenheim, Phys. Rev. B **15**, 4292 (1977).

[15]K. R. A. Ziebeck and P. J. Brown, J. Phys. F **10**, 2015 (1980).

[16]R. Résibois and C. Piette, Phys. Rev. Lett. **24**, 514 (1970).

[17]R. Folk and H. Iro, Phys. Rev. B **32**, 1880 (1985).